Title: Antibacterial activity of 3D versus 2D TiO_2 nanostructured surfaces to investigate curvature and orientation effects

Alka Jaggessar[a,b,*], S.W.M.A. Ishantha Senevirathne[a,b], Amar Velic[a,b] and Prasad KDV Yarlagadda[a,b]

[a] School of Mechanical, Medical and Process Engineering, Queensland University of Technology, 2 George Street, Brisbane, Australia 4000

[b] Centre for Biomedical Technologies, Queensland University of Technology, 2 George Street, Brisbane, Australia 4000

[*] Corresponding Author: Alka Jaggessar (alka.jaggessar@qut.edu.au)

Author email addresses:

S.W.M.A. Ishantha Senevirathne: s.senevirathne@hdr.qut.edu.au

Amar Velic: a2.velic@qut.edu.au

Prasad KDV Yarlagadda: y.prasad@qut.edu.au

Keywords: bactericidal surfaces, hydrothermal synthesis, nanostructured surfaces, surface curvature, surface orientation.

Abstract

Nanostructured surfaces have recently been established as a novel surface technology to alleviate health and industrial problems caused by bacterial biofilms. While fundamental research has advanced, nanostructure arrays have generally only been developed on 2D, flat substrates, and evaluated by incubating bacteria parallel to nanostructure direction. These circumstances do not reflect real-world surfaces which are often curved and randomly oriented with respect to sedimentation direction. Titanium dioxide nanostructures on 3D, hemisphere-shaped substrates were fabricated using hydrothermal synthesis, to investigate effects of curvature and orientation on bactericidal performance. 3D surfaces were 91% more efficient at resisting *Staphylococcus aureus* adhesion than 2D surfaces, and cells that did attach were killed with the same or higher efficiency after 1 and 3 hours exposure to nanostructured surfaces. This preliminary study establishes hydrothermal synthesis as a viable fabrication method of 3D bactericidal surfaces and provides insight into surface curvature and orientation impact on bactericidal efficiency.

Introduction

The rise of antibiotic resistant bacteria has received significant attention in the last decade [1]. Researchers have attempted to quell this growing problem through many strategies, such as altering pharmaceutical drugs, reducing the over-prescription of antibiotic medication, and investigating methods of bacterial deactivation. The past few years has seen significant research interest in bactericidal surfaces inspired by naturally occurring antibacterial surfaces [2, 3]. The antibiofouling and bactericidal behaviour exhibited by certain species cicada [3], dragonfly [4-7] and butterfly wings [8, 9] have been found to inhibit the growth and spread of bacterial infection. Since this discovery, researchers have made many attempts to replicate this behaviour onto various material substrates

using a range of fabrication methods including different forms of lithography [10-13], wet-etching [14] and hydrothermal synthesis. Applications for this technology range from the surface of medical implants [15, 16] and general hospital surfaces [14] to prevent bacteria spread and transmission, to ship hulls [17] and piping [18] to prevent biofouling.

Although progress has been made to fabricate bactericidal nanostructures on various materials [19-21], the majority of these studies have so far been conducted on flat, two-dimensional (2D) substrates. This is due to the limitations of several fabrication methods such as electron beam lithography and reactive ion etching, where flat substrate surfaces are required. In reality, however, most of the surfaces which stand to benefit from antibacterial nanostructuring (e.g., hospital doorknobs, and prosthetic joint heads) are three-dimensional (3D) shapes containing complex geometric features such as curvature. The ability to produce nanostructure arrays on such shapes has not been strongly demonstrated, and the influence of curvature and orientation on bactericidal efficacy of nanostructures not been characterised. Establishing this behaviour is crucial for potential implementation of this technology.

Investigating the role of orientation is particularly interesting, because it may also speak to the underlying forces which drive cell contact, deformation, and – ultimately - antibacterial activity on nanostructured surfaces [22, 23]. Many authors have proposed that this force is gravity– in other words, it is through weight that cells ultimately die on nanostructured surfaces [24-26]. This would imply that nanopillars must point parallel, and opposite, to the direction of sedimentation of the bacteria (i.e., “up”) in order to be effective. If true, the real-world applicability of nanostructures would be severely limited, because such an orientation cannot be guaranteed. Unfortunately, with predominantly only 2D flat samples being investigated in the literature, the influence of direction and orientation has not been properly scrutinised.

Accordingly, this study investigates the use of hydrothermal synthesis to produce nanostructured titanium dioxide topology on complex, hemisphere-shaped 3D surfaces. This method of fabrication was chosen for its cost and time effectiveness [27], ease, environmental friendliness and prospective scalability. Moreover, as it is a chemical-based process, as long as the substrate is completely submerged into the alkaline solution, all regions of the substrate will be able to react with the solution, regardless of geometry. Secondly, this study establishes the impact of substrate curvature and orientation on bactericidal efficiency, specifically against Gram-positive *Staphylococcus aureus* (*S. aureus*).

Materials and Methods

Sample Fabrication

Hemispherical Ti-6Al-4V samples with a diameter of 1.4 cm (curved surface area of 4 cm^2) were produced from a Ti-6Al-4V cylindrical rod using a CNC Lathe at the Design and Fabrication Research Facility at the Queensland University of Technology. Flat Ti-6Al-4V (medical grade 5) samples were cut to represent the same surface area (i.e., 2×2cm). All samples were sonicated in acetone for 10 minutes and rinsed thoroughly with 18.2 MΩ H_2O. To synthesise nanostructures, samples were reacted with 60 mL 1M NaOH in a 125 mL Parr acid digestion vessel at 180°C for 2 hours. After cooling to room temperature, samples were rinsed with 18.2 MΩ H_2O and dried using N_2 gas. Samples were then annealed in a furnace for 1 hour at 300°C and once cool, submerged in 0.6 M HCl for 30 minutes. After rinsing with 18.2 MΩ H_2O, samples were lastly calcined for 2 hours at 600°C.

Surface Characterisation

Following hydrothermal synthesis, the sample surfaces were characterised using a JEOL 7001F scanning electron microscopy (SEM) to visualise nanostructure morphology. Surface characterisation was performed using an accelerating voltage of 15eV and a probe current of 8mA. Flat surfaces have previously been characterised using nanoindentation, X-ray diffraction and contact angle [19, 28, 29] for mechanical, chemical and wettability properties, respectively. Due to the curved nature of the hemisphere samples, these tests were not completed one the curved surfaces however, since the hydrothermal fabrication process constant, it can be assumed that bulk mechanical, chemical and local wettability properties also remain constant.

Preparation of Bacterial Suspension

Colonies of *S. aureus* (ATCC 25923) were incubated in 5 mL of Nutrient Broth (Sigma Aldrich) for 16 hours and centrifuged at 5250 *× g* and 37°C for 5 minutes to separate the cells. These separated cells were resuspended in 1X Phosphate Buffered Saline (PBS) with turbidity of the suspension adjusted to 0.07923 ± 0.0065 OD_{600}, measured using a BioPhotometer (Eppendorf). The 2D and 3D samples were placed in microwells (6-microwell plate) with 5 mL of the bacterial suspension. Cells were incubated for 1 and 3 hours.

Live/Dead Fluorescence Assay

Following incubation, cells were stained with SYTO9 and propidium iodide (Live/Dead Baclight Kit, Invitrogen) mixed in a 1:1 ratio, and diluted to 1/100 with PBS. 15 µL of the dye mixture was pipetted onto each surface and incubated for a further 15 minutes in a dark room before substrates were retrieved and drained. Substrates were imaged using a Nikon Eclipse TiS fluorescence microscope using FITC and CY3 filters for live and dead cells, respectively. 20 images per sample were taken with 2 images in each location (i.e., with each of the two filters). All trials were repeated 3 times. Images were processed using ImageJ software to enhance contrast and binarized before counting the illuminated pixels. The illuminated pixel count on each image was taken as the surface coverage of bacterial cells.

SEM Visualisation of Bacteria-Surface Interaction

After fluorescence imaging, samples exposed to bacteria were prepared for SEM using standard biological protocol involving fixation, dehydration, drying and conductive coating. Accordingly, the samples were fixed using 3% glutaraldehyde ($C_5H_8O_2$), rinsed with 0.1 M cacodylate buffer and 1% OsT_4, dehydrated in a graded ethanol series (20 – 100%), dried with hexamethyldisiloxane ($C_6H_{19}NSi_2$) and sputter coated with 2nm platinum. High magnification (25-40k×) SEM imaging of the bacteria-surface interface and cell morphology was carried out under low accelerating voltage (5kV), spot size (8) and working distance (4mm) in order to probe surface signal with high resolution. The 2D, flat samples were mounted flat for imaging. The 3D, hemispherical samples however, were mounted at three different inclinations – 0° (flat), 45°, and 90° (perpendicular) – to image three different surface positions of interest.

Statistical Analysis

Statistical analysis for bacterial test results were completed using two-way ANOVA Tukey's multiple comparison test. Significant results are indicated in figures, where *p<0.1, **p<0.01, ***p<0.001 and ****p<0.0001.

Results and Discussion

When performed on a 3D, hemispherical sample, the hydrothermal method generated nanostructures near identical to those produced on a 2D, flat sample. Moreover, the nanostructures were able to conform to the curvature of the sample, growing approximately perpendicular to the surface. This phenomenon can be observed in Figure 1, which shows nanostructures – located halfway between the centre and the edge of the hemisphere – protruding at approximately 45°.

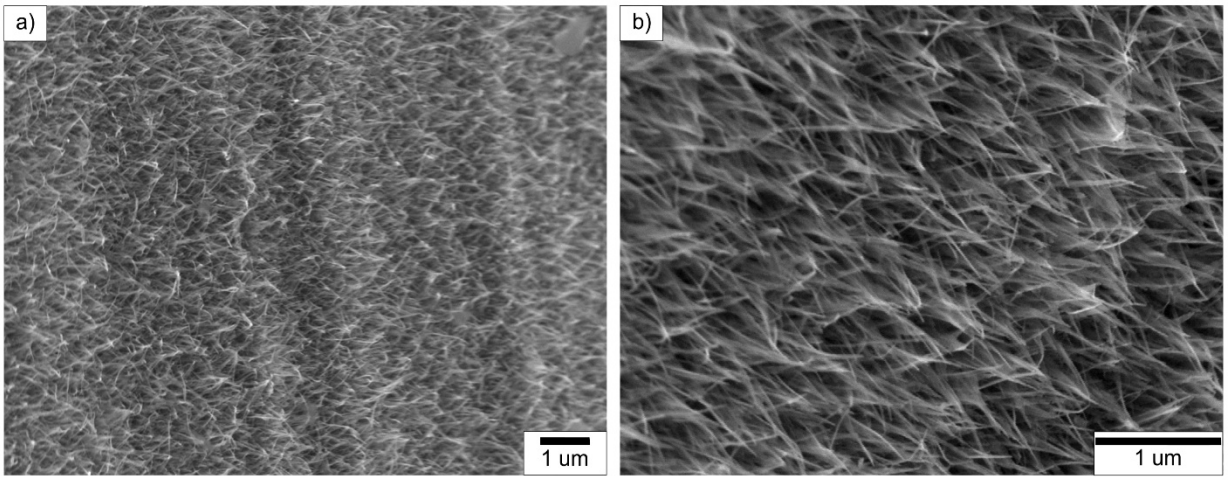

Figure 1: SEM images of hydrothermally synthesised TiO_2 structures fabricated on 3D, hemispherical samples. Images are taken at the midpoint between the centre and the edge of the sample.

Consistent with these observations, the antibacterial efficacy of the 3D, hemispherical sample was comparable to that of its 2D counterpart (Figure 2a-f). More specifically, the live/dead fluorescent assay revealed that the killing efficiency of the 3D surfaces was similar (1h incubation) or marginally higher (3h incubation) than that of the flat surface (Figure 2b). Impressively, whilst maintaining killing efficiency, the 3D surface also drastically reduced bacterial attachment (Figure 2a, c-f). For instance, attachment of live bacteria seen on a 204.14 × 165.12µm^2 after 3h incubation was reduced by 91% from 22 990 ± 4361 on flat surfaces to 2060 ± 247 cells on 3D surfaces (Figure 2a, e-f). Accordingly, application of the hydrothermal method on curved surfaces was overall favourable, as fewer cells adhered on the 3D surfaces (i.e., increased antibiofouling) and those that did were inactivated at the expected efficiency.

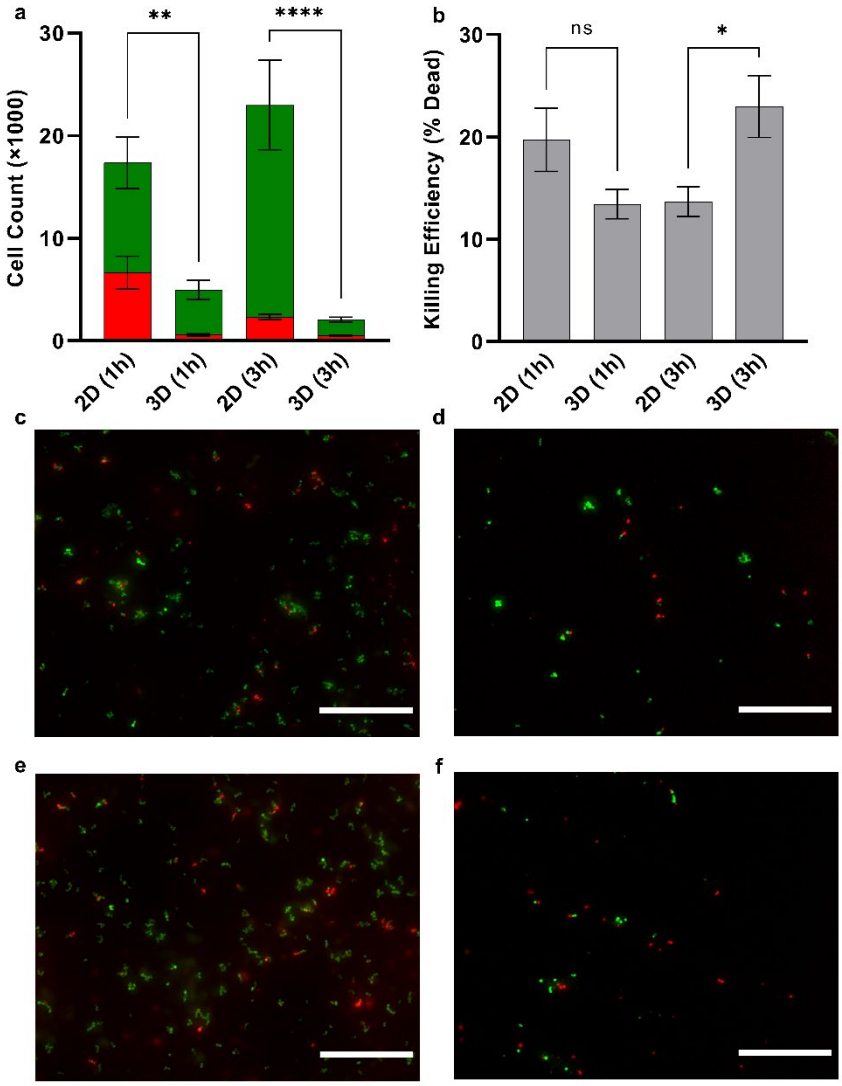

*Figure 2. Live/dead fluorescence assay to assess antifouling and killing efficiency of 2D, flat and 3D, hemispherical hydrothermal surfaces following 1h and 3h incubation in S. aureus suspension. a) Average number of live (green) and dead (red) S. aureus cells attached to the surfaces, observed within a 204.14×165.12μm^2 field. Statistical significance indicators correspond to the live cell counts, though the dead cell trends were also statistically significant. b) Average killing efficiency of each surface, quantified by counting the proportion of dead cells in fluorescence micrographs. Statistical significance is indicated where *p<0.1, **p<0.01, ***p<0.001 and ****p<0.0001. c-d) Composite fluorescence micrographs showing live (green, SYTO 9) and dead (red, PI) S. aureus cells after 1h incubation on the 2D and 3D hydrothermal surfaces, respectively. e-f) Composite fluorescence micrographs after 3h incubation on the 2D and 3D hydrothermal surfaces, respectively. All scale bars are 50μm.*

The antibacterial efficacy of the 3D, hydrothermal surfaces was further corroborated via qualitative observations made with SEM. In particular, the morphology of *S. aureus* cells attached to the hemispherical (Figure 3b-d) and flat (Figure 3a) surfaces was markedly similar. Both surfaces elicited two types of cell morphology: inflated, coccoid shape, consistent with viability; and, deflated, collapsed shape, consistent with death. The micrographs also qualitatively reinforced the increased antibiofouling behaviour of the 3D surface (Figure 3b-d), as there were fewer and less clustered *S. aureus* in comparison to the 2D surface (Figure 3a).

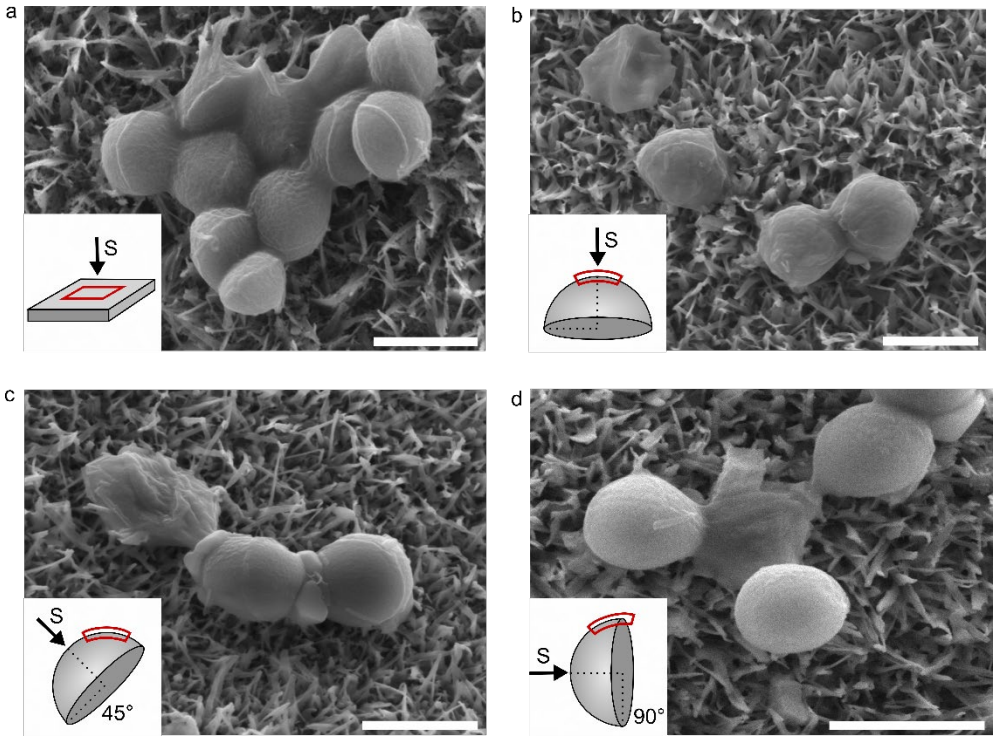

Figure 3. SEM investigation of S. aureus morphology and contact on 2D, flat and 3D, hemispherical hydrothermal surfaces after 3h incubation. a) Characteristic micrograph of S. aureus on 2D hydrothermal surface, where the direction of sedimentation is always parallel, and opposite, to the projection of nanostructures. b) Characteristic micrograph of S. aureus on 3D surfaces at top of hemisphere, where the direction of sedimentation is parallel, and opposite, to projection of nanostructures. c) Characteristic micrograph of S. aureus on 3D surfaces at side of hemisphere, where direction of sedimentation is at 45° to projection of nanostructures. d) Characteristic micrograph of S. aureus on 3D surfaces at edge of hemisphere, where direction of sedimentation is perpendicular (90°) to projection of nanostructures. Arrows denoted with 'S' indicate sedimentation direction during the initial bacterial incubation. Inserts show how samples were mounted in the SEM for imaging. All scale bars are 1µm.

The observation of deflated cells on 3D surfaces even where the direction of the nanostructures was perpendicular to the sedimentation direction (i.e., Figure 3d), suggests that gravity does not play an important role in the death process of the cell. At this location, due to the perpendicular orientation, the weight vector in the direction of the nanostructures is very small – theoretically, zero. As such, gravity cannot be driving the cells to sink into, and rupture on the nanostructures. Instead, this observation is more consistent with electromagnetic intermolecular forces, such as London-van der Waals, electric double layer, and acid-base, which act in all directions but tend to pull the cell towards the nearest surface. The present observation, taken together with the quantitative analysis in Velic et al [23] showing the negligible impact of cell weight, imply that gravity is not the driving force for antibacterial activity on nanostructured surfaces. This disagrees with the weight-based models proposed previously [24-26] but does reinforce intermolecular force-based models such as those by Pogodin et al [22] and Velic et al [23]. More importantly, the present findings overall bode well for the practical realisation of nanostructures surfaces, because – evidently – their efficacy is not eliminated by a change of orientation. More follow up investigations with creative experimental setups may be worthwhile in order to fully elucidate whether any detailed relationship exists between orientation and nanopattern bactericidal activity – that is, whether nanopattern bactericidal activity is, to any extent, anisotropic.

Conclusion

This work presented in this study show that TiO_2 nanostructures are achievable on non-flat substrate surfaces, using hydrothermal synthesis. Structures were observed to grow approximately

perpendicular to the substrate surface, indicating that hydrothermal synthesis is an appropriate method of nanostructure fabrication for complex shapes and surfaces. While both 2D and 3D surfaces show antibacterial properties against Gram-positive *S. aureus*, when compared to 2D surfaces, 3D surfaces exhibit improved antibiofouling properties. Furthermore, bacterial cells that do attach to 3D surfaces are killed with a 91% higher efficiency than those adhered to a 2D surface. This is a promising result and is a step towards the upscaling and implementation of this technology, to reduce bacterial transmission.

Acknowledgements

The authors would like to acknowledge the contribution and facilities used at the Central Analytical Research Facility and the Design and Fabrication Facility at Queensland University of Technology.

Author Contributions

AJ performed hydrothermal fabrication experiments on 2D and 3D surfaces and performed SEM characterisation of fabricated surfaces (and developed Figure 1), wrote various sections of the manuscript including abstract, introduction, conclusion and associated sections of the methodology, and formatted the manuscript for submission. SWMAIS designed and performed the live/dead fluorescence assay, wrote the corresponding methodology and developed Figure 2a,b, along with corresponding statistical analysis. AV performed SEM characterisation of bacteria on nanostructured surfaces, wrote the corresponding methodology, developed Figure 2c-f (including caption), developed Figure 3, wrote results and discussion, and contributed towards the introduction. PKDVY oversaw and supervised the study.

Funding

This research did not receive any specific grant from funding agencies in the public, commercial or not-for-profit sectors.

Annotated References

1. A. Velic, J. Hasan, Z. Li, P.K.D.V. Yarlagadda Mechanics of Bacterial Interaction and Death on Nanopatterned Surfaces. Biophys. J. 120 (2021) 217-231.

The formerly accepted model describing bacteria-nanostructure interaction and concomitant antibacterial activity was inter-pillar rupture, as proposed by Pogodin et al in 2013. The recent study by Velic et al., challenged this notion, by applying more accurate mechanical modelling to the problem (i.e., three-dimensional finite element modelling with carefully considered continuum mechanical properties, envelope structure, and adhesion interaction conditions). Velic et al. concluded that the pillar apex was the more critical action site of nanostructured surfaces, which has profound implications on how such surfaces should be designed.

2. S. Mimura, T. Shimizu, S. Shingubara, H. Iwaki, T. Ito Bactericidal effect of nanostructures: Via lytic transglycosylases of Escherichia coli. RSC Adv. 12 (2022) 1645-1652.

The work presented by Mimura et al is of special interest due to their focus on bacteria cell characteristics and the role it plays in bactericidal mechanisms of nanostructured surfaces. This is significant as the majority of studies attempting to describe the bacteria-structure interaction focus on the mechanical properties of the nanostructures. Mimura et al has shown that bacterial

cells experience autolysis during cell division of *E. coli*, explaining that most cell envelope damage was most likely to occur during cell division.

References

[1] E. Taylor, T.J. Webster Reducing infections through nanotechnology and nanoparticles. International journal of nanomedicine 6 (2011) 1463-1473.
[2] J. Hasan, A. Roy, K. Chatterjee, P.K.D.V. Yarlagadda Mimicking Insect Wings: The Roadmap to Bioinspiration. ACS Biomater. Sci. Eng. 5 (2019) 3139-3160.
[3] J. Hasan, H.K. Webb, V.K. Truong, S. Pogodin, V.A. Baulin, G.S. Watson, J.A. Watson, R.J. Crawford, E.P. Ivanova Selective bactericidal activity of nanopatterned superhydrophobic cicada Psaltoda claripennis wing surfaces. Appl. Microbiol. Biotechnol. 97 (2013) 9257-9262.
[4] C.D. Bandara, S. Singh, I.O. Afara, A. Wolff, T. Tesfamichael, K. Ostrikov, A. Oloyede Bactericidal effects of natural nanotopography of dragonfly wing on Escherichia coli. ACS Appl. Mater. Interfaces 9 (2017) 6746-6760.
[5] C.M. Bhadra, V.K. Truong, V.T.H. Pham, M. Al Kobaisi, G. Seniutinas, J.Y. Wang, S. Juodkazis, R.J. Crawford, E.P. Ivanova Antibacterial titanium nano-patterned arrays inspired by dragonfly wings. Sci. Rep. 5 (2015) 16817.
[6] D.E. Mainwaring, S.H. Nguyen, H. Webb, T. Jakubov, M. Tobin, R.N. Lamb, A.H.F. Wu, R. Marchant, R.J. Crawford, E.P. Ivanova The nature of inherent bactericidal activity: insights from the nanotopology of three species of dragonfly. Nanoscale 8 (2016) 6527-6534.
[7] C. Samuel, O. Stephanie, T. Vi Khanh, M. Denny, N. Soon Hock, V. Jitraporn, L. Denver, J.T. Mark, W. Marco, A.B. Vladimir, L. Pere, M. Richard, J. Saulius, J.C. Russell, P.I. Elena Pillars of Life: Is There a Relationship between Lifestyle Factors and the Surface Characteristics of Dragonfly Wings? ACS Omega 3 (2018) 6039-6046.
[8] G.D. Bixler, A. Theiss, B. Bhushan, S.C. Lee Anti-fouling properties of microstructured surfaces bio-inspired by rice leaves and butterfly wings. J Colloid Interface Sci 419 (2014) 114-133.
[9] Y. Fang, G. Sun Complex wettability and self-cleaning performance of butterfly wing surface. Appl Mech Mater 723 (2015) 943.
[10] H. Shahali, J. Hasan, H. Wang, T. Tesfamichael, C. Yan, P.K.D.V. Yarlagadda Evaluation of Particle Beam Lithography for Fabrication of Metallic Nano-structures. Procedia Manuf. 30 (2019) 261-267.
[11] J.-Y. Cho, G. Kim, S. Kim, H. Lee Replication of surface nano-structure of the wing of dragonfly (Pantala Flavescens) using nano-molding and UV nanoimprint lithography. Electron. Mater. Lett. 9 (2013) 523-526.
[12] A. Jaggessar, P. Yarlagadda, T. Qiu, T. Li, T. Tesfamichael Fabrication of Nano Pyramid Texture on Ti-6Al-4V Using Nanosphere Lithography. Mater. Today: Proc. 5 (2018) 11593-11600.
[13] G. Zhang, J. Zhang, G. Xie, Z. Liu, H. Shao Cicada wings: A stamp from nature for nanoimprint lithography. Small 2 (2006) 1440-1443.
[14] J. Hasan, Y. Xu, T. Yarlagadda, M. Schuetz, K. Spann, P.K.D.V. Yarlagadda Antiviral and Antibacterial Nanostructured Surfaces with Excellent Mechanical Properties for Hospital Applications. ACS Biomater. Sci. Eng. (2020)
[15] M. Jäger, H.P. Jennissen, F. Dittrich, A. Fischer, H.L. Köhling Antimicrobial and osseointegration properties of nanostructured titanium orthopaedic implans. Materials 10 (2017)
[16] J. Hasan, S. Jain, K. Chatterjee Nanoscale Topography on Black Titanium Imparts Multi-biofunctional Properties for Orthopedic Applications. Sci. Rep. 7 (2017) 41118.
[17] M. Salta, L. Capretto, D. Carugo, J.A. Wharton, K.R. Stokes Life under flow: A novel microfluidic device for the assessment of anti-biofilm technologies. Biomicrofluidics 7 (2013) 64118-64118.
[18] J.S. Vrouwenvelder, D.A. Graf von der Schulenburg, J.C. Kruithof, M.L. Johns, M.C.M. van Loosdrecht Biofouling of spiral-wound nanofiltration and reverse osmosis membranes: A feed spacer problem. Water Res. 43 (2009) 583-594.

[19] A. Jaggessar, A. Mathew, T. Tesfamichael, H. Wang, C. Yan, P.K. Yarlagadda Bacteria Death and Osteoblast Metabolic Activity Correlated to Hydrothermally Synthesised TiO2 Surface Properties. Molecules 24 (2019) 1201.
[20] T. Diu, N. Faruqui, T. Sjostrom, B. Lamarre, H.F. Jenkinson, B. Su, M.G. Ryadnov Cicada-inspired cell-instructive nanopatterned arrays. Sci. Rep. 4 (2014) 7122.
*[21] S. Mimura, T. Shimizu, S. Shingubara, H. Iwaki, T. Ito Bactericidal effect of nanostructures: Via lytic transglycosylases of Escherichia coli. RSC Adv. 12 (2022) 1645-1652.
[22] S. Pogodin, J. Hasan, V.A. Baulin, H.K. Webb, V.K. Truong, T.H. Phong Nguyen, V. Boshkovikj, C.J. Fluke, G.S. Watson, J.A. Watson, R.J. Crawford, E.P. Ivanova Biophysical model of bacterial cell interactions with nanopatterned cicada wing surfaces. Biophys. J. 104 (2013) 835-840.
*[23] A. Velic, J. Hasan, Z. Li, P.K.D.V. Yarlagadda Mechanics of Bacterial Interaction and Death on Nanopatterned Surfaces. Biophys. J. 120 (2021) 217-231.
[24] F. Xue, J. Liu, L. Guo, L. Zhang, Q. Li Theoretical study on the bactericidal nature of nanopatterned surfaces. J. Theor. Biol. 385 (2015) 1-7.
[25] M.J. Mirzaali, I.C.P. van Dongen, N. Tümer, H. Weinans, S.A. Yavari, A.A. Zadpoor In-silico quest for bactericidal but non-cytotoxic nanopatterns. Nanotechnology 29 (2018) 43LT02-43LT02.
[26] E. Maleki, M.J. Mirzaali, M. Guagliano, S. Bagherifard Analyzing the mechano-bactericidal effect of nano-patterned surfaces on different bacteria species. Surf. Coat. Technol. 408 (2021) 126782.
[27] A. Hayles, J. Hasan, R. Bright, D. Palms, T. Brown, D. Barker, K. Vasilev Hydrothermally etched titanium: a review on a promising mechano-bactericidal surface for implant applications. Materials Today Chemistry 22 (2021) 100622.
[28] A. Jaggessar, A. Mathew, H. Wang, T. Tesfamichael, C. Yan, P.K.D.V. Yarlagadda Mechanical, bactericidal and osteogenic behaviours of hydrothermally synthesised TiO2 nanowire arrays. J. Mech. Behav. Biomed. Mater. 80 (2018) 311-319.
[29] A. Jaggessar, T. Tesfamicheal, H. Wang, C. Yan, P.K.D.V. Yarlagadda Investigation of mechanical properties and morphology of hydrothermally manufactured titanium dioxide nanostructured surfaces. Procedia Manuf. 30 (2019) 373-379.